First-principles analysis of the electric structure, optical properties, and phonon transmission of a VTe monolayer in the rock-salt phase

Mustafa M. Jaafar
Department of Physics, College of Education for Pure Sciences, University of Basrah, Basrah
Corresponding Author: Tel.: +94-77-07398937
E-mail addresses: habw0604@gmail.com (Mustafa M. Jaafar)

Jabbar M. Khalaf Al-zyadi
Department of Physics, College of Education for Pure Sciences, University of Basrah, Basrah

ABSTRACT

First-principles simulations based on density functional theory (DFT) are used to examine the structural, electric, and optical properties of the (RS) VTe monolayer as well as the phonon transport. The (RS) VTe monolayer demonstrated distinct electric characteristics along with a wide absorption spectrum spanning the visible to ultraviolet range. Additionally, a decrease in its convergent phonon scattering rate was discovered. These results demonstrate the possibility for more theoretical and experimental studies of the electric, structure, optical properties, and thermal conductivity of the VTe monolayer. The results of the experiments have demonstrated that the monolayer of (RS) VTe has the property of being a half-metal. When the energy levels crossed the Fermi level in the spin-up position, the substance displayed metallic characteristics. In contrast, in the spin-down configuration, an energy gap appeared on both sides of the Fermi level, resulting in the creation of a semiconductor. This is shown by the presence of a gap between the conduction and valence bands, with the total energy gap of the compound determined by the sum of both gaps. The energy gap of the (RS) VTe monolayer was measured to be 0.7 eV, which is half the size of the energy gap of a typical metal (0.4 eV). Furthermore, the half-metal character of the (RS) VTe monolayer resulted in a magnetic moment per unit cell similar to 3μ_B revealing a significant polarization at the Fermi level.

Keywords: VBi; Half-metallic ferromagnetism; monolayer properties; DFT; optical characteristics

Introduction

The majority of current research has focused on half-metallic (HM) materials because of their indirect roles in the advancement of electronic device technology. The half-metallic properties of Heusler alloys are of great interest to spin-electronic device researchers. In 1983, De Groot and his team found these molecules in two half-Heusler compounds (NiMnSb and PtMnSb) [1-3]. Using a mechanical exfoliation technique, Konstantin Novoselov and his colleagues successfully isolated graphene from Craft in 2004. Due to the exceptional physical, magnetic, optical, mechanical, and electrical characteristics of ultra-thin 2D nanomaterials like graphene, this ground-breaking discovery created new opportunities in the field of nanomaterials [4,5]. Because of this, these nanomaterials have attracted unheard-of attention and are thought to have enormous potential in optical-electronic devices and a variety of applications, such as transistors, nanoscale devices, catalysts, nano electromechanics, photocatalysis, gas sensors, and optical detectors [6,7].Researchers have been particularly interested in a particular kind of half-metallic substance known as HM. Due to their electrical structure, these materials exhibit 100% spin

polarization at Fermi level, making them potential candidates for spin-link applications. The presence of numerous half-metallic ferromagnetic materials has been predicted and confirmed by thorough simulations over the past 35 years. The Moore Act, established in 1965 by Gordon Moore, one of Intel's pioneers, is responsible for this advancement in technology [8,9]. Moore noted that while chip prices stay constant, the number of transistors on a processing chip increases roughly every two years [10,11]. This discovery led Intel to combine silicon (Si) with integrated circuits, sparking a global technological revolution. Through the application of the quantum tunnelling effect principle, silicon, which has become the preferred material for microprocessors for more than four decades, has now reached the nanoscale. In the realm of materials science, considerable advancements have been achieved over time, including the discovery of full Heusler alloys and other half-metals (HM) [12]. Scientists are intrigued by these special molecules, also known as Heusler compounds, because of their remarkable qualities. Some of these alloys display features of both metals and semiconductors or insulators, according to further analysis of their electronic structure [13,14]. Due to this peculiar behavior, the phrase "half of the metal ferromagnetism" was created, which refers to the alloy's capacity to display ferromagnetism in just one spin direction. In recent years, significant efforts have been invested in developing reliable methods for producing 2D nanomaterials suitable for various applications [15-17]. Top-down and bottom-up strategies have both been thoroughly investigated. To create single-layer or low-layer two-dimensional nanomaterials, the top-down technique requires eliminating the van der Waals contact between stacked layers of bulk-layered crystals. This process has made great strides and been essential in the miniaturization of electronic devices like computers, tablets, and mobile phones. These developments have significantly enhanced the utility, dependability, and effectiveness of these technologies, completely altering how people live their lives [18].

Computational methods

This work used the CASTEP algorithm together with density functional theory to compute the optical, magnetic, electric, phonon transport, and structural properties of a (RS) VTe monolayer. [19]. These features include optical, magnetic, electric, and phonon transport. Generalised gradient approximations (GGA) and the PBE technique have been used to analyses the exchange-correlation energy [20]. In order to remove any potential atom-atom interactions, the constructed system is a (RS) VTe monolayer with 15 Å inserted in a direction perpendicular to the surface of the 2D monolayer. The constructed system is a (RS) VTe monolayer consisting of (2 × 2 × 1) per unit cell. The cutoff energy of 500 eV is used when examining plane waves. Every structure has attained its most relaxed state. The size of the atomic force is less than 0.02 eV/Å, but the magnitude of the total energy affinity is 10^{-5} eV. To replicate the structural, electric, magnetic, phonon transport, and optical properties of the (RS) VTe monolayer, a sample is collected from the first Brillouin zone using the coordinates (15 × 15 × 1).

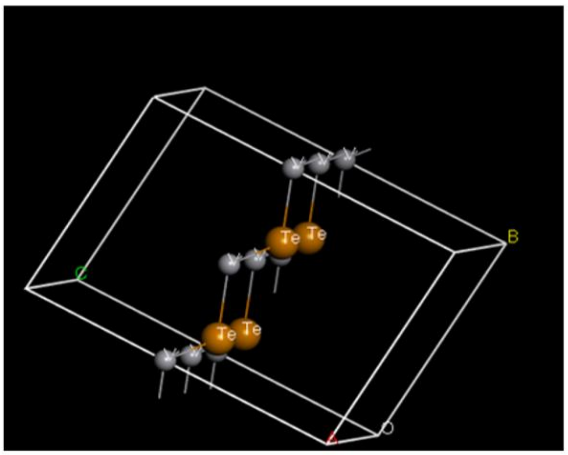

Fig. 1.Crystal structure of (RS) VTe monolayer

Results and discussion

3.1 Electronic structures of (RS) VTe monolayer

The Fermi level at the top of the half-metal gap (HMGap) in the equivalency package is 0.4 eV. Because (V) contains seven electrons that have crossed the E_F, two of which are in the s orbital and five of which are in the p orbital, it is more effective than (Te) [21].

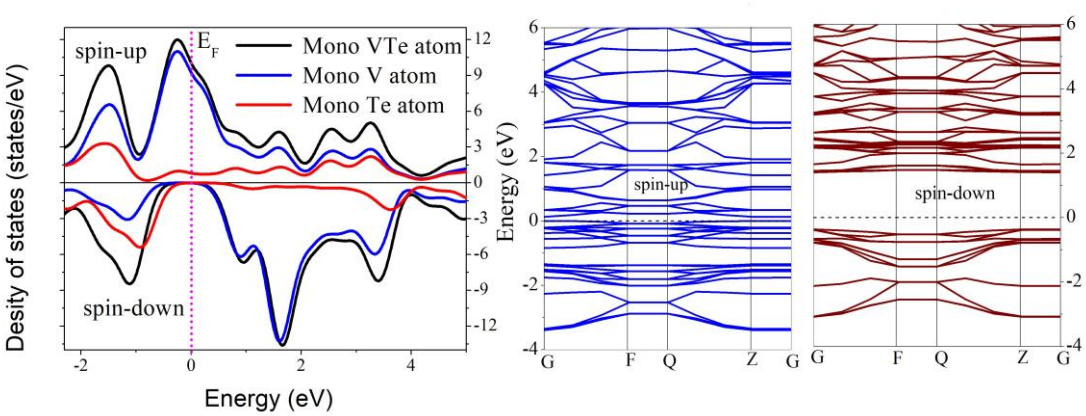

Fig. 2. The densities of states in the monolayer VTe (left) and the band structure (spin up and spin down) of VTe (right)

3.2 Phonon Transport

The necessity for a more thorough scientific knowledge of heat transmission through materials has been brought to light by recent advancements in the research of partly metallic materials. Density functional theory (DFT) simulations of first-principles calculations are a valuable technique for determining the scattering of phonons in the (RS) VTe monolayer. Materials physics must include the study of phonons. In reality, phonons are essential for generating a wide range of physical characteristics, such as thermal conductivity and electrical conductivity A phonon is, in other words, the lowest quantity of energy that can be transmitted from an auditory source to a physical medium. In this case, the phonon is analogous to an electromagnetic wave isotope, or the lowest quantity of electromagnetic energy that can be transmitted from an electromagnetic wave to a physical medium [22]. The phonon dispersions of the (RS) VTe monolayer are shown in Figure 3. Because the phonon dispersions do not have the imaginary vibrational frequency throughout the Brillouin region, the monolayer is dynamically stable.

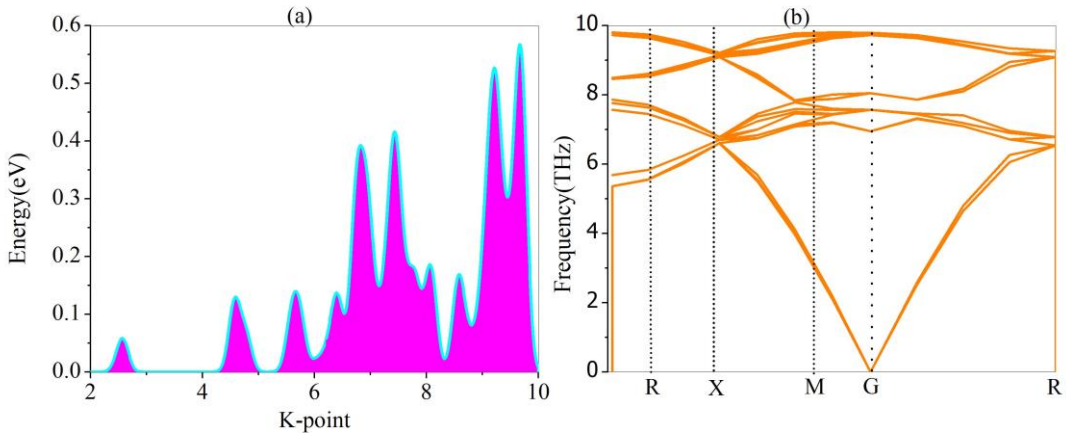

Fig. 3. Curves of phonon dispersion and state density of (RS) VTe monolayer.

3.3 Optical Properties

Due to their larger surface area for absorbing sunlight, two-dimensional materials have enhanced photovoltaic cells, accelerating the process of light conversion. Fundamental research and modern applications depend heavily on the optical properties of materials. Among other optical properties, we calculated the conductivity, dielectric function, loss function, refractive index, propagation constant (K), and absorption coefficient. Utilizing the relationship below, it is determined.

$$\varepsilon(\omega) = \varepsilon_1(\omega) + i\varepsilon_2(\omega) \quad (1)$$

where the imaginary and real components of the dielectric function are represented by the $\varepsilon_1(\omega)$ and $\varepsilon_2(\omega)$, respectively. The electromagnetic field's propagative conduct has a connection to reality $\varepsilon_1(\omega)$ [23]. The Fermi golden rule is used for adding the occupied–unoccupied transitions to obtain the relationship for the imaginary part $\varepsilon_2(\omega)$ [24]. Figure 4 depicts the real and imaginary parts of the dielectric function. The (RS) VTe monolayers has a dielectric function (at zero energy) of is 15×10^5 and 65×10^5. Additionally, the fact that the real dielectric function is not negative shows that the (RS) VTe monolayer behaves like a semiconductor in this frequency range. While the insulation curve in visible regions grows and lowers with energy, UV radiation drops rapidly with photon energy increase. It is commonly known that materials having gaps less than 1.8 eV perform well in infrared (IR) and visible light. As a result, the (RS) VTe monolayer will function as a visual material in the infrared and visible ranges [25].

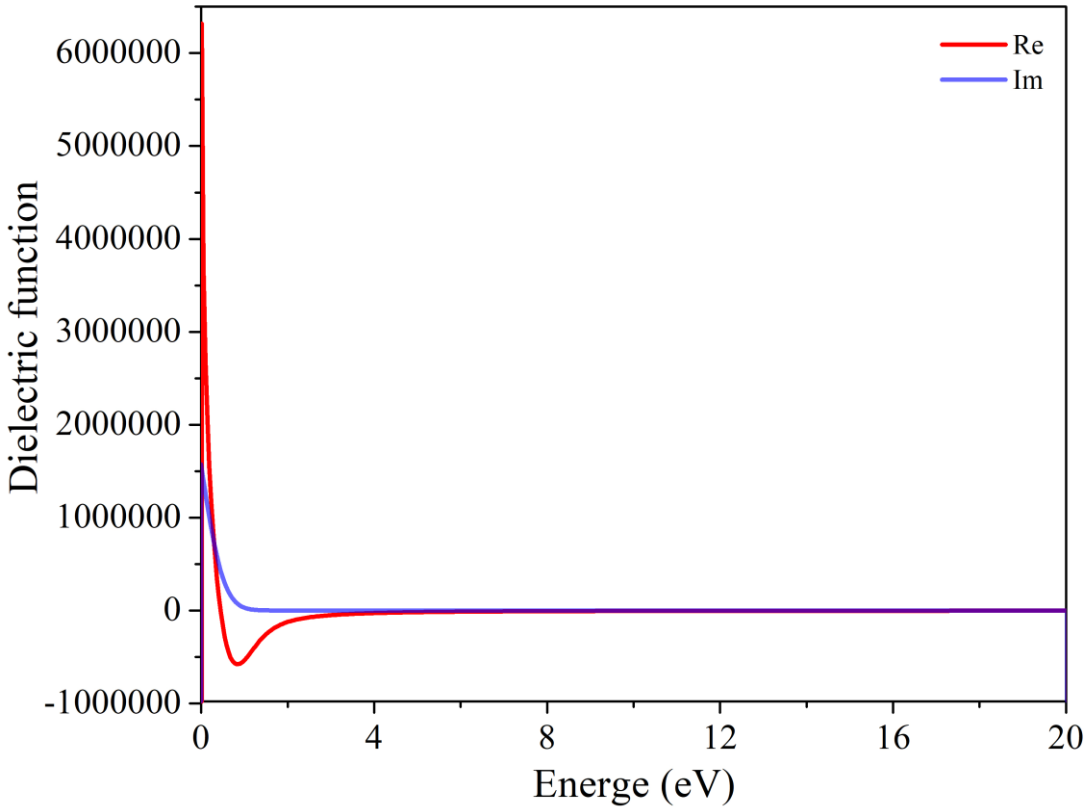

Fig. 4. Imaginary and real components of the dielectric function of the (RS) VTe monolayer

In the energy range of 0 to 20 eV, the optical characteristics were investigated. According to Figure 5, absorption in the infrared (IR) region begins at energies below 0.07 eV, and 1.3 eV for the (RS) VTe monolayer. Our findings supported the existence of an IR absorption peak between (0.8 eV and 1.3 eV). Its largest peaks are unmistakably in the UV (8 eV) region, according to the absorption coefficient. One of the most significant study topics on light absorption that may be employed in the production of solar cells is the absorption of visible light, which starts in the region between (1.5 eV and 3 eV). The high ultraviolet light absorption energy of a single layer of (RS) VTe monolayer, which may be employed in photoelectronic devices like UV detectors, is another finding.

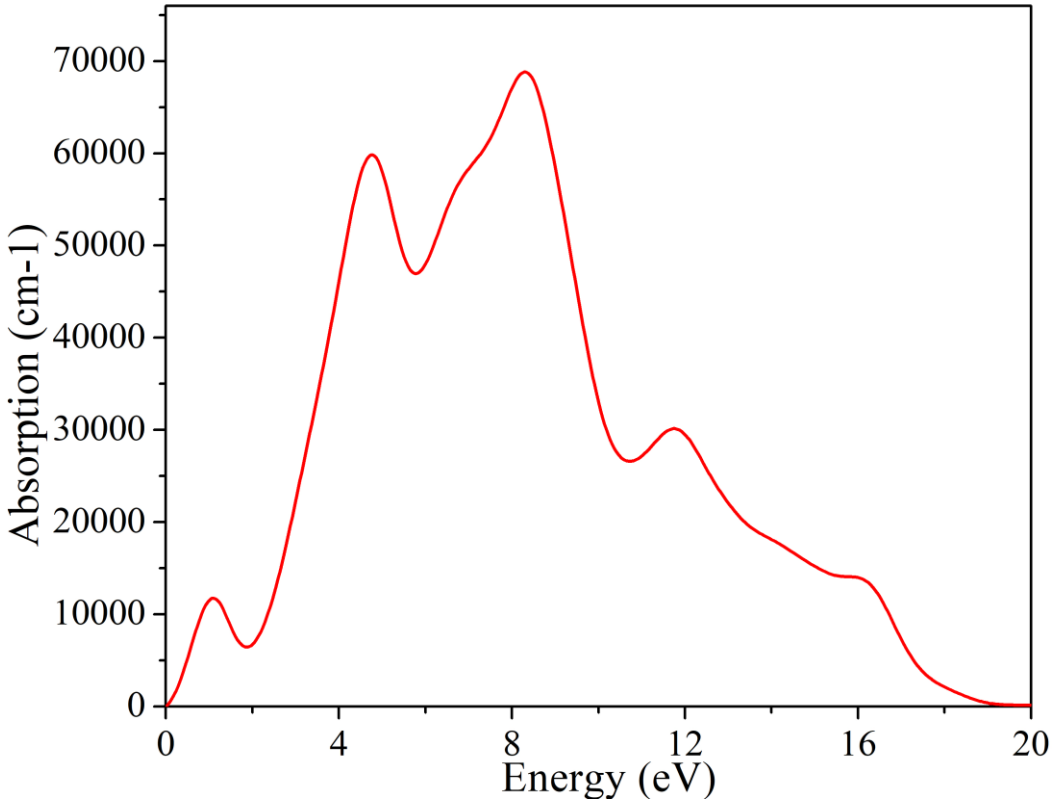

Figure 5: Optical absorption of (RS) VTe monolayer

Figure (6) shows the refractive index and propagation constant of the (RS) VTe monolayer as a function of photon energy. The propagation coefficient (at zero energy) and refractive index of the (RS) VTe monolayer are 7.9 and 1.9, respectively. On the other hand, the propagation constant has a maximum value of 2.9 at 2.5 eV. At high photon energies, the refractive index finally has a tendency to stabilise, but in the visible spectrum and with UV light, it tends to decrease with energy. In general, the monolayer's highest refractive index is in the infrared region. The spectra of the propagation constant (K) and the refractive index (n) quickly decline and stabilize at 20 eV for the photon.

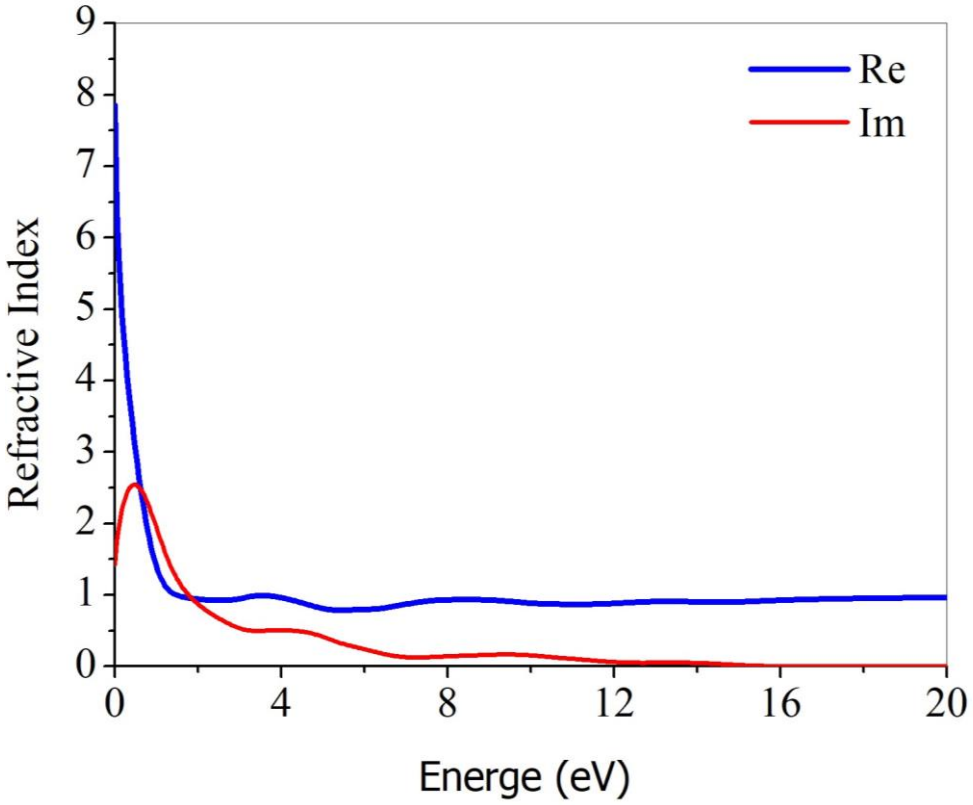

Figure 6: Refractive index and propagation constant of (RS) VTe monolayer

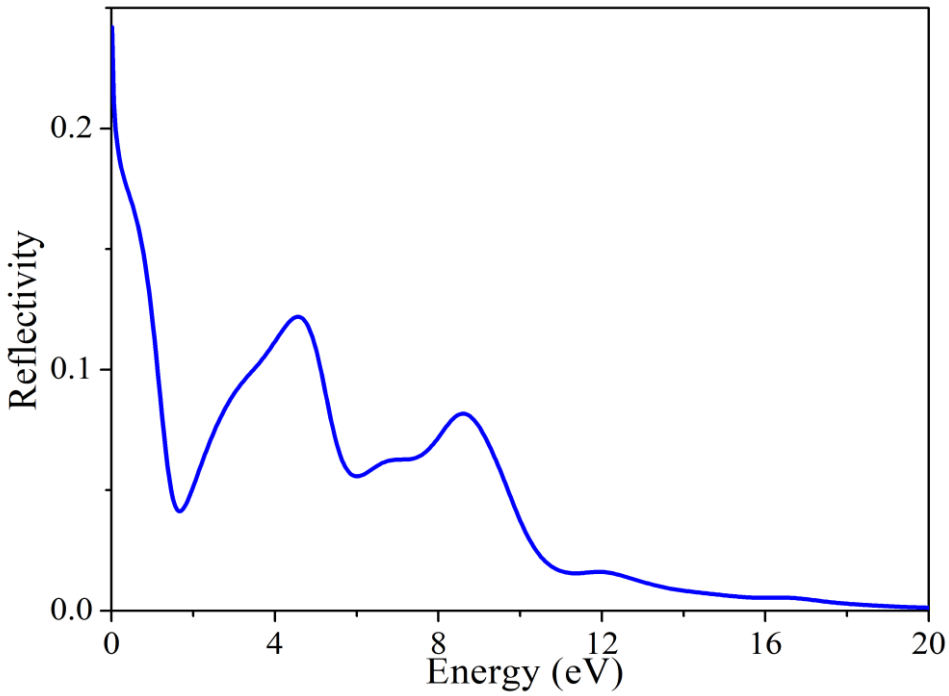

Figure 7: Reflectivity of (RS) VTe monolayer

The predicted optical reflectivity as a function of energy is shown in Figure 7. Optical reflectivity at the zero energy is 0.25 .At 4.5 eV, there is one optically reflective peak for photon energy. In visible light, the optical reflectivity curve falls with energy; in ultraviolet light, it falls quickly with increasing photon energy. From Figure 8, we notice that the highest peak of the loss function is at energy 10 eV and its value is 1.3.

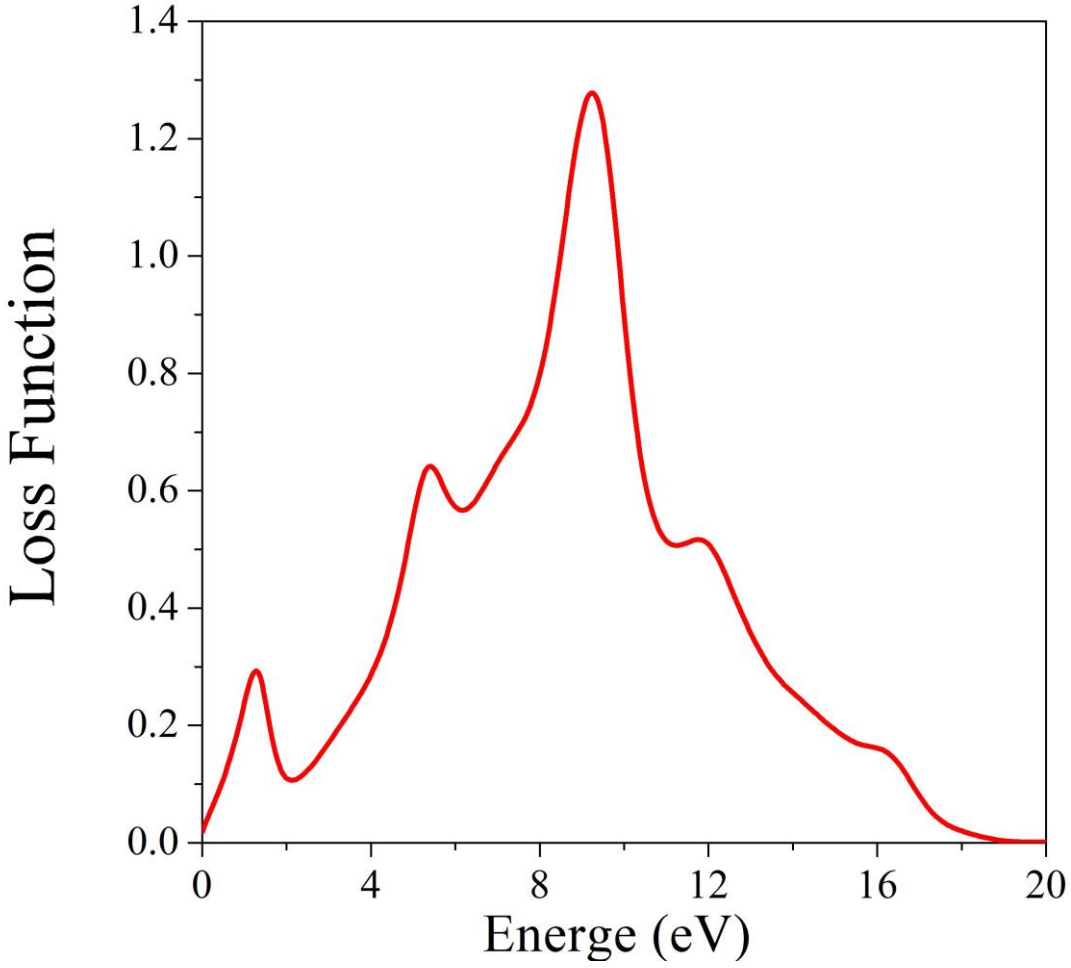

Figure 8: Loss function of (RS) VTe monolayer

Figure 9 shows optical conductivity as a function of photon energy. In the infrared region of 95000, the conductivity of the real part of the (RS) VTe monolayer clearly peaks at 1.3 eV. In contrast, at photon energies of 3 eV, the imaginary component of conductivity's maximum values in the visible ray zone are 65000.

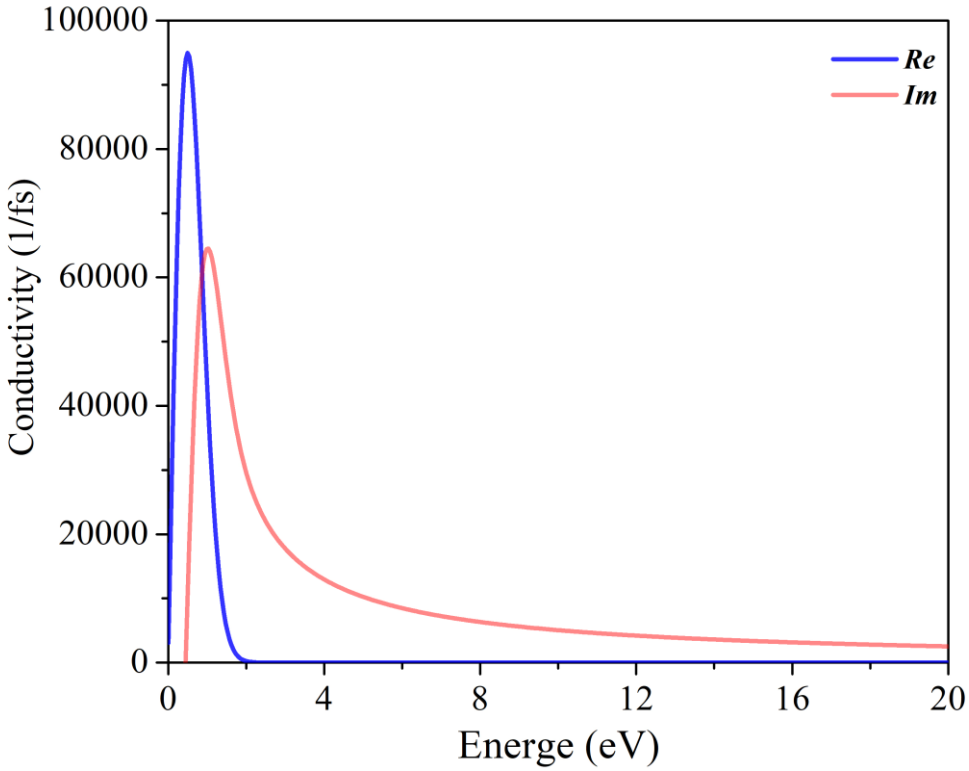

Figure 9: Optical conductivity of (RS) VTe monolayer

Conclusion

In this study, a first-principles analysis is used to examine the electrical structure, optical characteristics, and phonon transport of the (RS) VTe monolayer. The (RS) VTe monolayer exhibits half-metallic characteristics, showing that the spin-down channel is a semiconductor with an energy gap of 0.7 eV and the spin-up channel is metallic. that the (RS) VTe monolayer has an average magnetic moment of $3\mu_B$ per cell unit. The lack of fictitious phonon vibration frequencies over the whole Brillouin region contributes to the dynamic stability of the (RS) VTe monolayer as well. The (RS) VTe monolayer is a strong contender for employment in microelectronic and electro-optical applications, according to the researched optical properties.

References

[1] R. A. de groot, F. M. Mueller, P. G. Van Engen and K. H. J. Buschow, "New Class of Materals: Half-metallic Ferromagnets", phys. Rev. Lett. (1983), 50: 2024.
[2] J. H. Park, E. Vescovo, H. J. Kim, C. Kwon, R. Ramesh and T. Venkatesan, "Direct evidence for a half-metallic ferromagnet", Nature. (1998), 392: 794.
[3] M. I. Katsnelson, V. Yu. Irkhin, L. Chioncel, A. I. Lichtenstein and R. A. de Groot,"Half-metallic ferromagnets: From band structure to many-body effects", Rev. Mod. phys. (2008), 80: 315
[4] C. Felser, G. H. Fecher and B. Balke,"Spintronics: A Challenge for Materials Science and Solid-State Chemistry", Angew. Chem. Int. Ed. (2007), 46: 668.
[5] K. H. J. Buschow and P. G. van Engen, "Magnetic and magneto-optical properties of heusler alloys based on aluminium and gallium", J. Magn. Magn. Mater. (1981), 25 : 90
[6] R. Y. Umetsu, K. Kobayashi, R. Kainuma, Y. Yamaguchi and K. Ohoyama, A. Sakuma, K. Ishida,"Powder neutron diffraction studies for the L21 phase of Co2YGa (Y = Ti, V, Cr, Mn and Fe) Heusler alloys", J. Alloys Comp., (2010), 1:499.

[**7**] G. Y. Gao and K. L. Yao, "First-principles prediction of half-metallic ferromagnetism in five transition-metal chalcogenides: The case of rocksalt structure", J. Appl. Phys. (2012), 111: 113703.
[8] K.S. Novoselov, A.K. Geim, S. V Morozov, D.A. Jiang, Y. Zhang, S. V Dubonos, I.V Grigorieva, and A.A. Firsov, Electric field effect in atomically thin carbon films, Science 306 (2004) 666.
[9] A.K. Geim, K.S. Novoselov, The rise of graphene, Nanosci. Technol. 11 (2009) 19.
[10] H.R. Jappor, Electronic structure of novel GaS/GaSe heterostructures based on GaS and GaSe monolayers, Phys. B. Condens. Matter. 524 (2017) 109.
[11] H.R. Jappor, Electronic and structural properties of gas adsorbed graphene-silicene hybrid as a gas sensor, J. Nanoelectron. Optoelectron. 12 (2017) 742.
[12] X. Chen, R. Meng, J. Jiang, Q. Liang, Q. Yang, C. Tan, X. Sun, S. Zhang, and T. Ren, Electronic structure and optical properties of graphene/stanene heterobilayer, Phys. Chem. Chem. Phys. 18 (2016) 16302.
[13] H.R. Jappor, and A.S. Jaber, Electronic properties of CO and CO2 adsorbed silicene/graphene nanoribbons as a promising candidate for a metal-free catalyst and a gas sensor, Sens. Lett.15 (2016) 14.
[14] H.R. Jappor, S.A.M. Khudair, Electronic properties of adsorption of CO, CO2, NH3, NO, NO2 and SO2 on nitrogen doped graphene for gas sensor applications, Sens. Lett.15 (2017) 432.
[15] X.W.Z. Cheng, K. Xu, H.K. Tsang, and J.-B. Xu, High-responsivity graphene/silicon-heterostructure waveguide photodetectors, Nat. Photonics. 7 (2013) 888.
[16] K.R. Paton, E. Varrla, C. Backes, R.J. Smith, U. Khan, A. O'Neill, C. Boland, M. Lotya, O.M. Istrate, and P. King, Scalable production of large quantities of defect-free few-layer graphene by shear exfoliation in liquids, Nat. Mater. 13 (2014) 624.
[17] G. E. Moore, Cramming more components onto integrated circuits, Electronics, 38 (1965) 8.
[18] M.M. Waldrop, The chips are down for Moore's law, Nature. 12 (2016) 144.K.S. Novoselov, A.K. Geim, S. V Morozov, D.A. Jiang, Y. Zhang, S. V Dubonos, I.V Grigorieva, and A.A. Firsov, Electric field effect in atomically thin carbon films, Science 306 (2004) 666.
[1**9**] S.J. Clark, M.D. Segall, C.J. Pickard, P.J. Hasnip, M.I. Probert, K. Refson, M.C. Payne, First principles methods using CASTEP. Z. Kristallogr. Cryst. Mater. 220 (2005) 567.
[20] J.P. Perdew, K. Burke, M. Ernzerhof, Phys. Rev. Lett. 77 (1996) 3865.
[20] Wang, J. Yu, J. Supercond. Nov. Magn. 31 (2018) 2789.
[22] PHONONS 2007: 12th International Conference on Phonon Scattering in Condensed Matter. 3 (2005) 140.
[23] M. Gajdoš, K. Hummer, G. Kresse, J. Furthmüller, F. Bechstedt, Phys. Rev. B 73 (2006) 045112.
[24] G.Y. Guo, K.C. Chu, D.S. Wang, C.G. Duan, Phys. Rev. B 69 (2004) 205416.
[25] D.K. Sang, B. Wen, S. Gao, Y. Zeng, F. Meng, Z. Guo, and H. Zhang, Nanomaterials 9 (2019) 1075